

Piotr P. Goldstein¹

A study on the Belinski-Khalatnikov-Lifshitz scenario through quadrics of kinetic energy

*1

¹*Theoretical Physics Division National Centre for
Nuclear Research, Pasteura 7, Warsaw, Poland*
(Dated: November 13, 2024)

arXiv:2411.07846v1 [math-ph] 12 Nov 2024

¹ email: piotr.goldstein@ncbj.gov.pl

Abstract

A detailed description of the asymptotic behaviour in the Belinski-Khalatnikov-Lifshitz (BKL) scenario is presented through a simple geometric picture. The Lagrangian version of the dynamics governed by the BKL equations is described in terms of trajectories inside a conical subset of the corresponding space of the generalised velocities. The calculations confirm that the initial conditions of decreasing volume inevitably result in total collapse, while oscillations along paths reflecting from a hyperboloid, similar to Kasner's solutions, occur on the way. The exact solution, found in our previous work, proves to be the only one that shrinks to a point along a differentiable path. Therefore, its instability means that the collapse is always chaotic. The collapse of the universe along asymptotics of exact Kasner's solutions is proved to be impossible for solutions of the BKL equations.

CONTENTS

I. Introduction	3
II. Earlier results	4
A. Origin of the equations	4
B. Basic properties of the equations	4
C. The exact solution	5
III. Methods	6
A. Useful variables	6
B. The cone of kinetic energy	8
IV. Solutions ending in the apex of the cone	11
A. The exact solution in the cone	11
B. On the possibility of other solutions ending in the apex	11
V. Solutions ending on the surface of the cone	12
A. Asymptotics of the diagonal velocities	12
B. Impossibility of the exact Kasner-like asymptotics	13
C. Quasi-Kasner solutions	13
VI. Conclusions	14
A. Proof that the exact solution is the only differentiable approach to all-direction collapse	16
B. Proof that all trajectories eventually tend to the apex	17
References	18

I. INTRODUCTION

The Belinski-Khalatnikov-Lifshitz scenario [1] was an answer to an important question: do the Einstein equations have solutions which describe the universe tending to (or stemming from) a cosmic singularity, for a considerable set of initial (or, respectively final) conditions? If they do, what is the behaviour of the universe in the neighborhood of the singularity?

Rather than “considerable” the authors used the term “generic solution”, as corresponding to a subset having nonzero measure in the space of initial (or final) conditions of the proper dimensionality (equivalently: with the proper number of arbitrary constants).

The equations in question read

$$\frac{d^2 \ln a}{dt^2} = \frac{b}{a} - a^2, \quad \frac{d^2 \ln b}{dt^2} = a^2 - \frac{b}{a} + \frac{c}{b}, \quad \frac{d^2 \ln c}{dt^2} = a^2 - \frac{c}{b}, \quad (1)$$

subject to the constraint

$$\frac{d \ln a}{dt} \frac{d \ln b}{dt} + \frac{d \ln a}{dt} \frac{d \ln c}{dt} + \frac{d \ln b}{dt} \frac{d \ln c}{dt} = a^2 + \frac{b}{a} + \frac{c}{b}. \quad (2)$$

Here $a = a(t)$, $b = b(t)$ and $c = c(t)$ are the so-called directional scale factors proportional to length scales in the synchronous reference system, while the time parameter t is the proper time rescaled by the volume scale (zero of the proper time corresponds to the limit $t \rightarrow \infty$ if the initial state has zero volume). The evolution of the scale factors defines the dynamics of the characteristic lengths in three principal directions while the universe tends to the singularity. Due to time-reversibility of equations (1)–(2), they may describe both expansion of the universe starting from the singularity and its final collapse. In this paper, we consider the asymptotics $t \rightarrow \infty$.

Numerous papers, were devoted to the analysis (both analytic and numeric) of the asymptotic behaviour of the universe in the BKL scenario, e.g. [1–4]. A Hamiltonian approach was analyzed in detail in [5], and a comparison with the diagonal mixmaster universe was done in [6]. The scenario was discussed in detail, on a broad background of related Bianchi models, in the book by Belinski and Henneaux [7]. Compared to those analyses, the goal of this paper is rather modest: we provide a simple geometric picture, which yields some useful exact results on the BKL scenario, staying within physics described by the BKL equations (1), (2). Relatively little attention has been devoted to the possibilities inherent in the equations themselves. Exact solutions (6) were not known until the author’s work with Piechocki [8]. Recently, other explicit solutions were found for special cases, where a or b/a , or c/b are equal to zero [9]. It seemed to be very likely that a more detailed analysis of the equations (1), (2), could yield interesting results about their solutions and consequently on physics of the universe in the described regime. This analysis is performed in this paper, with the stress on the asymptotic behaviour near the singularity. It includes the question of the chaotic character of the approach to the singularity, which was first discussed in [10]. In this paper, we provide a rigorous proof that the exact solution (6) is the only one which is differentiable down to the limit $t \rightarrow \infty$. Since this solution was found to be unstable in [8], it means that the approach according to the BKL equations is always chaotic.

This paper is structured as follows:

In section II, the earlier results are shortly summarised. These include the origin of the equations (1), (2), and their basic properties, as well as the exact solution from [8]. Section III contains description of methods, especially the geometric tool of the present analysis,

which is the cone of the kinetic part of the Lagrangian (further called “kinetic energy”). Section IV contains (in IV B) one of the main results, which is uniqueness of the exact solution (6) as the only one which allows for the collapse of the universe having differentiable length scales. In Section V, the Kasner-like and quasi-Kasner solutions are described. The other main result, stating that the BKL equations do not allow for asymptotics of the exact Kasner solutions, is discussed in Subsection V B.

Lengthy proofs have been postponed to two appendices.

II. EARLIER RESULTS

A. Origin of the equations

The details of the derivation of the BKL equations were described in a concise way in [3]. To summarise, the authors of BKL choose a special coordinate system for the Einstein equations in the special frame of reference, and make simplifying assumptions which they expect to be satisfied in the neighbourhood of the singularity. The chosen frame of reference is the synchronous one, in which the time is the proper time at each point; this reduces the dynamics to a problem of finding a 3-dimensional (3D) metric with time-dependent parameters. Symmetries of such systems were analyzed in detailed by Bianchi, the most general case being Bianchi VIII and IX models, which apply to this case. In the 3-dimensional space, a coordinate system is also specified.

The main simplifications are [1]: (1) assumption that the influence of matter on the metric may be neglected if we are sufficiently close to the singularity, and (another assumption) (2) that a typical initial anisotropy would grow indefinitely while approaching the singularity. Under these assumptions, the rotation of the principal axes in the given spatial frame (obtained from 3 off-diagonal spatial-spatial components of the Einstein equations) slows down to zero on the approach to the singularity. From the diagonal spatial-spatial components of the Einstein equations, three equations (1) follow in the limit of infinite anisotropy. The variables a , b and c of (1) are, up to constants of order 1, the time-dependent components of the spatial metric tensor in the three principal directions. This way, they define squares of the spatial scales. The temporal-temporal Einstein equation yields the constraint (2), while three spatial-temporal Einstein equations influence the values of constants, but do not contribute to the dynamics. The independent variable t in (1), (2) is the proper time rescaled by $dt = dt_{\text{proper}}/\sqrt{\gamma}$, where γ is the determinant of the spatial metric tensor (and $\sqrt{\gamma}$ defines the volume scale).

B. Basic properties of the equations

Symmetries: In the equations, (1), (2), there is no symmetry under permutation of a , b and c . On the contrary, the growing anisotropy assumption results in $a \gg b \gg c$. The system is symmetric under time reversal $t \rightleftharpoons -t$; thus it can describe the universe in both a collapse or an explosion as its reversal. The equations have two Lie symmetries [11]: the first is shift in time $t \rightleftharpoons t - t_0$ for any t_0 (which is obvious for an autonomous system). The second is a scaling symmetry: If a , b and c constitute the solution of (1), (2), and λ is the scaling parameter, $t' = \lambda t$, $a' = a/\lambda$, $b' = b/\lambda^3$, $c' = c/\lambda^5$, then a' , b' and c' as functions of t' make another solution of the system.

Dependence: The system is apparently overdetermined, due to the constraint (2) imposed on solutions of (1). However, the constraint specifies a value of the only constant of motion. Therefore, each of the equations (1) may be obtained from a system consisting of the other two of (1) and the constraint (2). E.g. [11], if we substitute \ddot{a} and \ddot{b} from the first two of the equations (1) into the t -derivative of the constraint (2), we obtain the 3rd equation of (1) multiplied by $(\dot{a}/a + \dot{b}/b)$ (the dot denotes time differentiation). This way, the 3rd equation is shown to be dependent on the other two of (1) and the constraint (2), with the exception of solutions satisfying $ab = \text{const}$ (which is consistent with equations (1), (2) for trivial $a = b = 0$ only).

Canonical structure [5] Substitution

$$a = \exp(x_1), \quad b = \exp(x_2), \quad c = \exp(x_3) \quad (3)$$

yields a system derivable from a Lagrangian

$$\mathcal{L} = \dot{x}_1\dot{x}_2 + \dot{x}_2\dot{x}_3 + \dot{x}_3\dot{x}_1 + \exp(2x_1) + \exp(x_2 - x_1) + \exp(x_3 - x_2), \quad (4)$$

with the constraint (2) turning into [5]

$$\mathcal{H} := \sum_{i=1}^3 \frac{\partial \mathcal{L}}{\partial \dot{x}_i} \dot{x}_i - \mathcal{L} = \dot{x}_1\dot{x}_2 + \dot{x}_2\dot{x}_3 + \dot{x}_3\dot{x}_1 - \exp(2x_1) - \exp(x_2 - x_1) - \exp(x_3 - x_2) = 0. \quad (5)$$

Equation (5) clarifies the sense of the dependence between (1) and (2): the constraint (2) is a particular choice of the first integral \mathcal{H} for solutions of equations (1), namely $\mathcal{H} = 0$.

The Lagrangian has a well defined potential and kinetic “energies”. The latter is an indefinite quadratic form of signature $(+, -, -)$, whose zero surface is a cone. As seen from (5), the potential energy is always negative while the total energy is zero. This means that the kinetic energy is positive, i.e., position of the system in the space of “velocities” is inside the cone (further the quotation marks will be omitted, also for the accelerations, i.e., derivatives of the velocities, and also for the kinetic, potential and total energies).

C. The exact solution

In [8], we found an exact analytical solution of the BKL equations. The solution is unique up to a time shift. It reads

$$a(t) = \frac{3}{|t - t_0|}, \quad b(t) = \frac{30}{|t - t_0|^3}, \quad c(t) = \frac{120}{|t - t_0|^5} \quad (6)$$

where $|t - t_0| \neq 0$ and t_0 is an arbitrary real number.

The exact solution may be obtained by a substitution of a Laurent series about an arbitrary singular point t_0 , or by looking for a solution which has power-like behaviour for $t \rightarrow \infty$, or else as a self-similar solution with respect to the scaling symmetry mentioned in subsection 2.2 [8].

Instability of the exact solution In [8], we explicitly solved the linear equation for small perturbations of the exact solution and we found that the exact solution is unstable. The perturbations have two oscillatory components whose amplitudes tend to zero as $t \rightarrow \infty$, but it is insufficient for stability, as the scale factors a , b , c also tend to zero. The instability

manifests in the growth of the ratios of the perturbation amplitudes to the respective perturbed scale factors; these ratios increase as $t^{\frac{1}{2}}$. A characteristic value of the ratio between the oscillation frequencies (approximately equal to 2.06) is one of the results of [8]; some chance exists that this ratio might have left marks in the spectrum of presently observed waves.

If we consider expansion of the universe from a point, the oscillations grow with time, but their growth is slower by the factor $t^{-1/2}$ than the expansion. Hence, with respect to the expansion itself, we can consider the expanding universe as stable (the terms proportional to K_3 in equation (16) of [8], though apparently increasing, represent time shift only).

Importance of the exact solution The reader might consider the exact solution unimportant: it requires very special initial conditions and it is unstable. However, it will later be proved that it is the only differentiable solution of the BKL equations in which the collapse to zero occurs in all three principal directions. The fact that the only solution suitable for a model of the universe smoothly collapsing to a point is unstable seems to be an important property of the BKL equations.

III. METHODS

We apply the aforementioned Lagrangian formalism, and illustrate the evolution of the system by its trajectory in the space of velocities in the diagonalised version of Lagrangian (4) (defined in the first subsection).

A. Useful variables

Transformation (3) naturally replaces the original variables a, b, c by their logarithms x_1, x_2, x_3 , suitable for the Lagrangian description. However, the description becomes clearer if we diagonalise the kinetic energy. If we care about simplicity of the equations rather than unitarity of the diagonalising transformation (accepting its determinant to be -6), a good substitution is

$$x_1 = u_1 - u_2 - u_3, \quad x_2 = u_1 + 2u_3, \quad x_3 = u_1 + u_2 - u_3, \quad (7)$$

which yields the Lagrangian in the form diagonal in the velocities $\dot{u}_1, \dot{u}_2, \dot{u}_3$,

$$\mathcal{L} = 3\dot{u}_1^2 - \dot{u}_2^2 - 3\dot{u}_3^2 + \exp(2(u_1 - u_2 - u_3)) + \exp(u_2 - 3u_3) + \exp(u_2 + 3u_3). \quad (8)$$

Variables u_1, u_2, u_3 define the principal directions in the velocity space. The dynamics in the new variables is determined by the Lagrange equations

$$\ddot{u}_1 = \frac{1}{3}e^{2(u_1 - u_2 - u_3)}, \quad (9a)$$

$$\ddot{u}_2 = e^{2(u_1 - u_2 - u_3)} - e^{u_2} \cosh(3u_3), \quad (9b)$$

$$\ddot{u}_3 = \frac{1}{3}e^{2(u_1 - u_2 - u_3)} - e^{u_2} \sinh(3u_3). \quad (9c)$$

with the constraint

$$\mathcal{H} := 3\dot{u}_1^2 - \dot{u}_2^2 - 3\dot{u}_3^2 - e^{2(u_1 - u_2 - u_3)} - 2e^{u_2} \cosh(3u_3) = 0. \quad (9d)$$

In terms of the original variables, the new ones are

$$u_1 = \frac{1}{3} \ln(abc), \quad u_2 = \frac{1}{2} \ln(c/a), \quad u_3 = \frac{1}{6} \ln(b^2/ac). \quad (10)$$

As we can see, u_1 is the logarithm of the volume scale, up to a multiplicative constant. Hence, the orthogonalisation automatically separates dynamics of the volume from that of the shape, thus doing what Misner introduced in the first stage of his transformation for the mixmaster model [12].

The velocities might simply be expressed in terms of the canonical momenta $p_i = \partial\mathcal{L}/\partial\dot{u}_i$, $i = 1, 2, 3$; then \mathcal{H} becomes the Hamiltonian, whose kinetic part is also a diagonal quadratic form in the momenta. However, the momenta are equal to the velocities, up to a multiplicative constant. Therefore, we do not introduce extra momentum-variables.

The variables u_1, u_2, u_3 will be extensively used in our further analysis.

Variables a, b, c are not suitable for numerical simulations, especially for their graphic presentation, because of the disproportion between their sizes $a \gg b \gg c$. This purpose is better served by quantities of equal order of magnitude. The shape of equations (1) and (2) suggest that these could be

$$q := a^2, \quad r := b/a, \quad s := c/b, \quad (11)$$

while their logarithmic counterparts

$$y_1 := \ln q, \quad y_2 := \ln r, \quad y_3 := \ln s, \quad (12)$$

would be the counterparts of x_1, x_2, x_3 for the corresponding Lagrangian description. A simple manipulation of the original equations (1) leads to those satisfied by the new variables, which may be cast into a compact form

$$\begin{pmatrix} \ln q \\ \ln r \\ \ln s \end{pmatrix}'' = M \cdot \begin{pmatrix} q \\ r \\ s \end{pmatrix}, \quad \text{or} \quad \begin{pmatrix} \ddot{y}_1 \\ \ddot{y}_2 \\ \ddot{y}_3 \end{pmatrix} = M \cdot \begin{pmatrix} e^{y_1} \\ e^{y_2} \\ e^{y_3} \end{pmatrix} \quad (13)$$

with the constraint given by

$$\frac{1}{2} (\ln q \ \ln r \ \ln s)' \cdot M^{-1} \cdot \begin{pmatrix} \ln q \\ \ln r \\ \ln s \end{pmatrix}' - q - r - s = 0 \quad (14)$$

where the constant matrix M is given by

$$M = \begin{pmatrix} -2 & 2 & 0 \\ 2 & -2 & 1 \\ 0 & 1 & -2 \end{pmatrix}, \quad \text{with} \quad \det M = 2, \quad M^{-1} = \begin{pmatrix} \frac{3}{2} & 2 & 1 \\ 2 & 2 & 1 \\ 1 & 1 & 0 \end{pmatrix}. \quad (15)$$

Equations (13) for y_i , $i = 1, 2, 3$ may be derived from a simple Lagrangian

$$\mathcal{L} = \frac{1}{2} (\dot{y}_1 \ \dot{y}_2 \ \dot{y}_3) \cdot M^{-1} \cdot \begin{pmatrix} \dot{y}_1 \\ \dot{y}_2 \\ \dot{y}_3 \end{pmatrix} + e^{y_1} + e^{y_2} + e^{y_3} \quad (16)$$

The constraint again corresponds to $\mathcal{H} = 0$, where \mathcal{H} differs from the Lagrangian (16), by the opposite signs at the exponential functions. Explicitly

$$\mathcal{H} = \frac{3}{4}\dot{y}_1^2 + 2\dot{y}_1\dot{y}_2 + \dot{y}_2^2 + \dot{y}_2\dot{y}_3 + \dot{y}_3\dot{y}_1 - (e^{y_1} + e^{y_2} + e^{y_3}) = 0. \quad (17)$$

Diagonalisation of the kinetic energy in the Lagrangian (16), is achieved by substitution of y_1 , y_2 and y_3 with their values in terms of u_1 , u_2 and u_3 respectively

$$y_1 = 2(u_1 - u_2 - u_3), \quad y_2 = u_2 + 3u_3, \quad y_3 = u_2 - 3u_3, \quad (18)$$

which leads back to Lagrangian (8) and the constrained Lagrange equations which stem from it (9).

B. The cone of kinetic energy

Our basic geometric tool for analysis and presentation of the dynamics will be the quadrics of kinetic energy.

$$E_k := 3\dot{u}_1^2 - \dot{u}_2^2 - 3\dot{u}_3^2 = \epsilon \geq 0. \quad (19)$$

For $\epsilon > 0$ they are two-sheet hyperboloids, becoming a cone for $\epsilon = 0$. Assume that the initial conditions describe a universe, whose volume is decreasing. In the variables \dot{u}_1 , \dot{u}_2 and \dot{u}_3 , we have

Proposition 1. *The dynamics of the universe which shrinks with t takes place in the lower interior of the cone*

$$3\dot{u}_1^2 - \dot{u}_2^2 - 3\dot{u}_3^2 > 0, \quad \dot{u}_1 < 0. \quad (20)$$

Proof. The first inequality (*interior*) follows from the constraint (9d), from which $3\dot{u}_1^2 - \dot{u}_2^2 - 3\dot{u}_3^2$ is equal to a sum of exponential functions and hence it is positive. The second (*lower*, i.e. $\dot{u}_1 < 0$) is equivalent to the assumption that the volume scale is decreasing, by the first equation of (10). \square

The following properties make the cone of kinetic energy a particularly useful tool, reproducing essential information that phase diagrams provide for single functions:

Proposition 2. *The conical surface $3\dot{u}_1^2 - \dot{u}_2^2 - 3\dot{u}_3^2 = 0$ is a singular surface of the solution.*

Proof. From the constraint (9d), if the kinetic energy E_k turns to zero, then the sum of exponential functions (the minus potential energy, E_p) also has to be zero, whence all exponents in (18) tend to $-\infty$ on approach to the surface (including its apex). This requires that at least u_1 and u_2 tend to $-\infty$. \square

Proposition 3. *The position of the system in the cone, together with the direction of the tangent to the trajectory, provide complete information on the local values of u_1 , u_2 , u_3 and their time derivatives.*

Proof. The Cartesian coordinates of the position in the cone are the components of the velocity, \dot{u}_1 , \dot{u}_2 and \dot{u}_3 . The direction of the tangent yields proportions between the components of the acceleration \ddot{u}_1 , \ddot{u}_2 and \ddot{u}_3 . Given the components of the velocity, the length of the acceleration vector can be retrieved from

$$2\ddot{u}_2 - 9\ddot{u}_1 + 3\dot{u}_1^2 - \dot{u}_2^2 - 3\dot{u}_3^2 = 0, \quad (21)$$

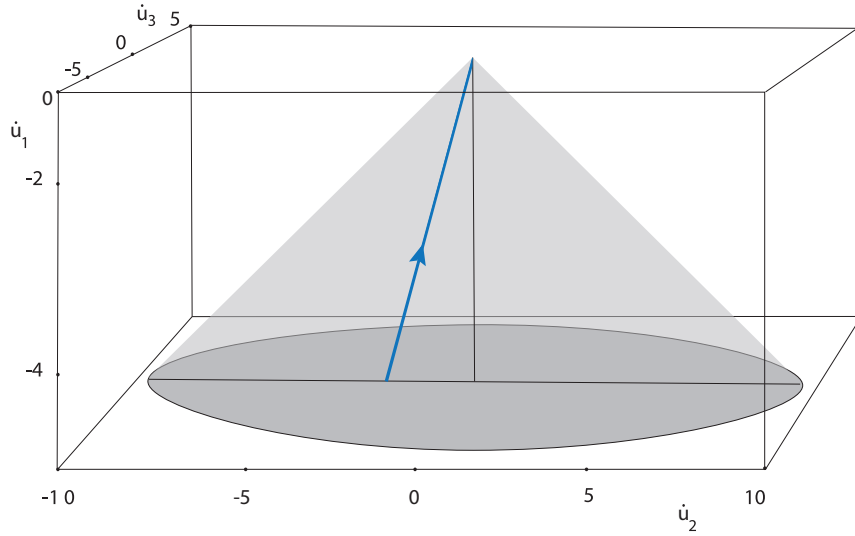


FIG. 1. The lower half (=shrinking volume) of the cone $3\dot{u}_1^2 - \dot{u}_2^2 - 3\dot{u}_3^2 > 0$. The dynamics of the system takes place inside the cone. The blue line shows the exact solution; the arrow indicates its direction of evolution. For $t \rightarrow \infty$, the line tends to the apex of the cone.

A position in the cone, together with the tangent to the trajectory, provide complete information on u_1, u_2, u_3 , and their derivatives.

which is a simple linear combination of equations (9a), (9b) and (9d) (with the exception, $\ddot{u}_2/\ddot{u}_1 = 9/2$, which is possible only on the conical surface). Having the accelerations, we can calculate the values of u_1, u_2 and u_3 by solving the system (9a), (9b), (9c) for these variables.

By differentiation of these equations, we can obtain higher derivatives of u_i $i = 1, 2, 3$ if they exist. \square

Proposition 4. *Each of the velocities, \dot{u}_1, \dot{u}_2 and \dot{u}_3 , has a finite limit as $t \rightarrow \infty$.*

Proof. Solving the dynamics equations (9a), (9b), (9c), with respect to the exponential functions (including the components of the hyperbolic ones), we get

$$3\ddot{u}_1 = e^{2(u_1 - u_2 - u_3)}, \quad (22a)$$

$$4\ddot{u}_1 - \ddot{u}_2 - \ddot{u}_3 = e^{u_2 + 3u_3} \quad (22b)$$

$$2\ddot{u}_1 - \ddot{u}_2 + \ddot{u}_3 = e^{u_2 - 3u_3} \quad (22c)$$

The r.h.s. of these equations are positive, whence their l.h.s. are second derivatives of convex functions, and first derivatives, of increasing functions, $\dot{u}_1, 4\dot{u}_1 - \dot{u}_2 - \dot{u}_3$ and $2\dot{u}_1 - \dot{u}_2 + \dot{u}_3$, respectively. The latter functions are bounded, because the increasing property of \dot{u}_1 ,

together with $\dot{u}_1(0) < 0$, infer $|\dot{u}_1(t)| < |\dot{u}_1(0)|$, while both $|\dot{u}_2(t)|$ and $|\dot{u}_3(t)|$ are not greater than $\sqrt{3}|\dot{u}_1(t)|$ as long as we are inside the cone. Hence, all three linear combinations of the first derivatives have finite limits.

The determinant of the coefficient matrix in the l.h.s. of (22) is nonzero ($= 6$), whence limits $g_1 := \lim_{t \rightarrow \infty} \dot{u}_1$, $g_2 := \lim_{t \rightarrow \infty} \dot{u}_2$ and $g_3 := \lim_{t \rightarrow \infty} \dot{u}_3$ may be uniquely calculated from the limits of these linear combinations. \square

Corollary 1. *From this result, it follows that $g_1 < 0$, $|g_2| \leq \sqrt{3}|g_1|$, $|g_3| \leq |g_1|$ and*

$$u_1 \sim g_1 t, \quad u_2 \sim g_2 t, \quad u_3 \sim g_3 t \text{ as } t \rightarrow \infty. \quad (23)$$

Corollary 2. *As y_i , $i = 1, 2, 3$ are linear combinations of \dot{u}_i (18), they also have finite limits as $t \rightarrow \infty$. However, for all i , $y_i \rightarrow -\infty$, which is a consequence of the constraint (17).*

Proposition 5. *A trajectory which ends on the surface or apex of the cone, needs infinite time to reach it.*

Proof. Consider a trajectory beginning in the lower half of the cone and ending on its surface or apex. Since, $\dot{u}_1 < 0$, hence u_1 is a decreasing function of time. On this basis, time may be calculated as

$$t = \int_{u_1(0)}^{u_1} du'_1 / \dot{u}'_1 \quad (24)$$

We have $0 > \dot{u}_1(t) \geq \dot{u}_1(0)$ in the lower half of the cone, whence $1/\dot{u}_1(t) \leq 1/\dot{u}_1(0) < 0$. Hence the integrand $1/\dot{u}'_1$ is separated from 0 in the interval of integration. On the other hand, $u_1 \rightarrow -\infty$ when we approach the boundary (see the proof of Proposition 2). The integral (24) in the limit $u_1 \rightarrow -\infty$ extends over infinite interval, while its integrand is separated from zero. Hence, it is infinite. \square

Remark. *The time calculated in (24), over a finite or infinite interval, is always positive, as the integrand is negative, while the lower limit of integration is greater than the upper limit.*

Proposition 6. *In the limit $t \rightarrow \infty$, each trajectory reaches the surface or apex of the cone.*

Proof. Time can also be expressed as

$$t = \int_{\dot{u}_1(0)}^{\dot{u}_1} d\dot{u}'_1 / \ddot{u}'_1, \quad (25)$$

because \dot{u}_1 is an increasing function of t (from (9a), commented in the proof of Proposition 4). For any point of the lower interior of the cone, the denominator is greater than zero (from (9a)), whence the integrand is finite and so are the limits of integration. Hence t has a finite value. Only at the surface or apex of the cone can t become infinite. \square

Remark. *Variable \dot{u}_1 may in principle replace time as it is an increasing function. Nevertheless, its use for this purpose is limited, as its variation is very uneven. There are time intervals where the exponential function in (9a) is close to zero and thus \dot{u}_1 hardly increases; also the other exponential components in (9) are very small (see Fig. 2, 3), and the trajectory comes very close to the surface of the cone. We call this behaviour “quasi-Kasner” and discuss it in subsection VC.*

Proposition 7. *There is no possibility of a stop in the interior of the cone (i.e., each point in the interior corresponds to nonzero acceleration).*

Proof. This property follows directly from equation (21). As long as $3\dot{u}_1^2 - \dot{u}_2^2 - 3\dot{u}_3^2 > 0$, we have $2\ddot{u}_2 - 9\ddot{u}_1 < 0$, which requires at least one nonzero component of the acceleration. \square

Remark. *Note the absence of \ddot{u}_3 in (21), which suggests that solutions with $\dot{u}_3 = 0$ may exist. Indeed, this is the case of the exact solution (26).*

Situations where the trajectory in the velocity space slows down to almost full stop may happen (see Fig. 2), which corresponds to the “quasi-Kasner” behaviour discussed in Subsection V C.

IV. SOLUTIONS ENDING IN THE APEX OF THE CONE

A. The exact solution in the cone

In terms of the u_i variables, the exact solution reads

$$u_1 = \frac{1}{3} \ln \frac{10800}{|t - t_0|^9}, \quad u_2 = \frac{1}{2} \ln \frac{40}{|t - t_0|^4}, \quad u_3 = \frac{1}{6} \ln \frac{5}{2}. \quad (26)$$

Obviously, for a given sign of $t - t_0$, both \dot{u}_1 and \dot{u}_2 have a simple pole, while $\dot{u}_3 = 0$. We also have $\dot{u}_2 = \frac{2}{3}\dot{u}_1$, which means that the trajectory corresponding to the exact solution is a straight line whose one end is at the apex of the cone (see Fig. 1). Physically, it describes a power-like collapse of all scale factors a, b, c to zero, i.e. a collapse of the universe, in all directions, to a point, as $t \rightarrow \infty$ (if we reverse the time, it may be expansion of the universe from a point).

The instability of the exact solution found in [8] and mentioned in subsection II C, affects also the solution in terms of u_i , only the coefficients are different. However, the solution itself is regular up to the apex.

B. On the possibility of other solutions ending in the apex

A question arises: are there any other paths which approach the apex from the inner cone, along a regular (more precisely, differentiable) curve, apart from that of the exact solution?

The result is negative. Namely

Proposition 8. *The path in the cone, corresponding to the asymptotic of the exact solution (26), i.e.*

$$\dot{u}_1 \sim -\frac{3}{t - t_0}, \quad \dot{u}_2 \sim -\frac{2}{t - t_0}, \quad \dot{u}_3 \sim 0, \quad (27)$$

is the only one which approaches the apex from the lower interior of the cone along a differentiable curve.

The above result means that other integral curves ending at the apex do not approach it at any definite angle with the axis of the cone. Together with the instability of the exact solution, this implies that all-direction collapse of the universe must be chaotic.

The well-defined angle is equivalent to existence of finite limits

$$\lim_{t \rightarrow \infty} \ddot{u}_2/\ddot{u}_1 \quad \text{and} \quad \lim_{t \rightarrow \infty} \ddot{u}_3/\ddot{u}_1. \quad (28)$$

To represent the collapsing universe, the trajectory should be within the lower interior of the cone, defined by the inequalities (20). This imposes another constraint on the values of the limits (28). Namely

$$\lim_{t \rightarrow \infty} \left[\frac{1}{3} \left(\frac{\dot{u}_2}{\dot{u}_1} \right)^2 + \left(\frac{\dot{u}_3}{\dot{u}_1} \right)^2 \right] = \lim_{t \rightarrow \infty} \left[\frac{1}{3} \left(\frac{\ddot{u}_2}{\ddot{u}_1} \right)^2 + \left(\frac{\ddot{u}_3}{\ddot{u}_1} \right)^2 \right] = \leq 1. \quad (29)$$

The proof of the negative result is lengthy, therefore, it is put off to Appendix A.

V. SOLUTIONS ENDING ON THE SURFACE OF THE CONE

From the fact that \dot{u}_1 increases, we conclude that it has to approach the apex (as the exact solution) or the lateral surface of the cone. In this section, we discuss the latter case.

A. Asymptotics of the diagonal velocities

Let a trajectory end on the conical surface, not at the apex. Then, according to Proposition 4, all three velocities have their limits, $\dot{u}_i \rightarrow g_i$, $i = 1, 2, 3$ which satisfy the equation of the cone

$$3g_1^2 - g_2^2 - 3g_3^2 = 0 \quad (30)$$

With $\dot{u}_i \rightarrow g_i$, the asymptotic behaviour of the diagonal variables is $u_i \sim g_i t$. Translating equation (30) into asymptotics of the scale factors, according to (10), we obtain

$$a \sim \exp(2p_1 t), \quad b \sim \exp(2p_2 t), \quad c \sim \exp(2p_3 t) \quad (31)$$

where the common coefficient in front of p_i , $i = 1 - 3$ may have any value, depending on the time scale. Equation (30) turns into a constraint on the constants p_i

$$p_1 p_2 + p_2 p_3 + p_3 p_1 = 0, \quad (32)$$

which by rescaling of t so that $p_1 + p_2 + p_3 = 1$ (first Kasner's condition [12]) is equivalent to

$$p_1^2 + p_2^2 + p_3^2 = 1, \quad (33)$$

which is the second Kasner's condition, in accordance with [3]. Equation (32) implies that at least one and at most two of p_1, p_2, p_3 are positive. This means that a solution whose trajectory ends on the conical surface would behave as exact Kasner's solutions: the universe is squeezed to zero in one or two directions while being stretched to infinity in the remaining two or one.

B. Impossibility of the exact Kasner-like asymptotics

We are going to show that the exact Kasner-like solutions, though predicted and described in [3], cannot exist in the framework of the BKL equations. We will prove it in two stages, using the y_i , $i = 1, 2, 3$ variables of (12) (which are connected with the scale factors by (11) and with the u_i through (18)). Stage 1

Proposition 9. *Let $\gamma_1, \gamma_2, \gamma_3$ be the limits of $\dot{y}_1, \dot{y}_2, \dot{y}_3$ (respectively) at $t \rightarrow \infty$. Then $\gamma_1 = \gamma_2 = 0$, while $\gamma_3 \leq 0$.*

Proof. If for $t \rightarrow \infty$, the trajectory approaches the surface of the cone, then the kinetic part in the constraint (17) turns to zero. In terms of the limits γ_i

$$\frac{3}{4}\gamma_1^2 + 2\gamma_1\gamma_2 + \gamma_2^2 + \gamma_2\gamma_3 + \gamma_3\gamma_1 = 0 \quad (34)$$

The constraint (17) requires that the potential part also turns to 0. This means that the asymptotics $y_i = \gamma_i t + o(t)$, $i = 1, 2, 3$ has all $\gamma_i \leq 0$. To also satisfy (34), the first two of the γ 's must be zero. \square

Corollary 3. *For trajectories ending at the surface but not at the apex, we would have $\gamma_3 < 0$ (exactly), as vanishing of all three \dot{y}_i 's corresponds to the apex.*

Stage 2 Further limitation on γ_i follows directly from the dynamic equations (13) in their version expressed in terms of y_1 , y_2 and y_3 .

Proposition 10. *The only possible asymptotic behaviour of solutions to (13), which satisfies constraint (17), corresponds to $\gamma_1 = \gamma_2 = \gamma_3 = 0$.*

Remark. *This means that all solutions eventually end at the apex, i.e., the fate of the universe is a total collapse to a point (with reversed time – universe starts from a point). Moreover, together with Proposition 8, it means that the collapse is always chaotic.*

The proof is lengthy and therefore it has been put off to Appendix B.

C. Quasi-Kasner solutions

Although exact Kasner solutions do not exist, numerical calculations show that approximate Kasner-like solutions are possible. Namely, the trajectories may approach the surface of the cone and bounce at a short distance from it, thus switching the universe to what may be considered the next Kasner epoch. The trajectory then passes through the cone until it approaches another point on its surface, at a less negative value of \dot{u}_1 as this coordinate may only increase, according to (22a). As the cone narrows, the amplitude of this quasi-periodic oscillations diminishes. This behaviour corresponds to reflections from the potential walls on Misner's diagrams [12], while the surfaces of the corresponding quadrics (lower halves of the two-sheet hyperboloids)

$$3\dot{u}_1^2 - \dot{u}_2^2 - 3\dot{u}_3^2 = \epsilon_n \quad (35)$$

play the role of the equipotentials. The parameter n indexes a quadric at n -th reflection while ϵ_n is a measure of its closeness to the surface of the cone.

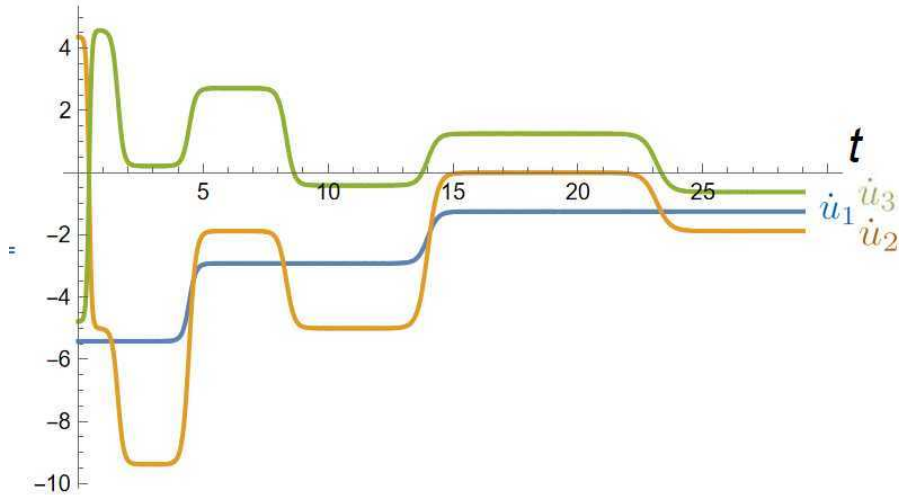


FIG. 2. Three components of the velocity \dot{u}_1 , \dot{u}_2 and \dot{u}_3 as functions of time parameter t . Each of them has time intervals of apparently constant values and there are intervals in which all three seem to be constant. Revealing their variability requires a logarithmic scale, as seen on the next figure.

Since the volume scale is proportional to $\exp(\frac{3}{2}u_1)$, while the time derivative, \dot{u}_1 , is negative throughout the evolution, the universe becomes more compact at subsequent reflections, although the reduction need not concern the scales in all directions.

Apparently, the velocity components \dot{u}_i remain constant for some time and the kinetic energy looks as if it were equal to zero. A logarithmic scale is necessary to reveal the actual variation of these quantities, as may be seen on fig. 3. This is due to the exponential dependence of the derivatives on the values of these variables.

VI. CONCLUSIONS

- We have analysed details of the possible dynamics of the universe while it undergoes contraction according to the BKL equations (1), (2). Due to reversibility of the equations, this may as well provide info on the beginning of our universe and the direction of its initial evolution. However, it does not include quantum effects like inflation.
- The asymptotics $t \rightarrow \infty$ may be oscillatory, but (unlike previously predicted), limits at $t \rightarrow \infty$ exist for all scale factors, their derivatives and first logarithmic derivatives. However
- The reflections from the potential walls in the Misner's picture, corresponding to reflections from a surface of a hyperboloid in our picture, eventually lead to all-direction collapse of the universe, due to the result of Proposition 10.
- The only asymptotic at $t \rightarrow \infty$ of this total collapse in which the approach is along a differentiable path it is the exact solution (6) (see Proposition 8. This shows exceptional role of the exact solution, in spite of its instability.

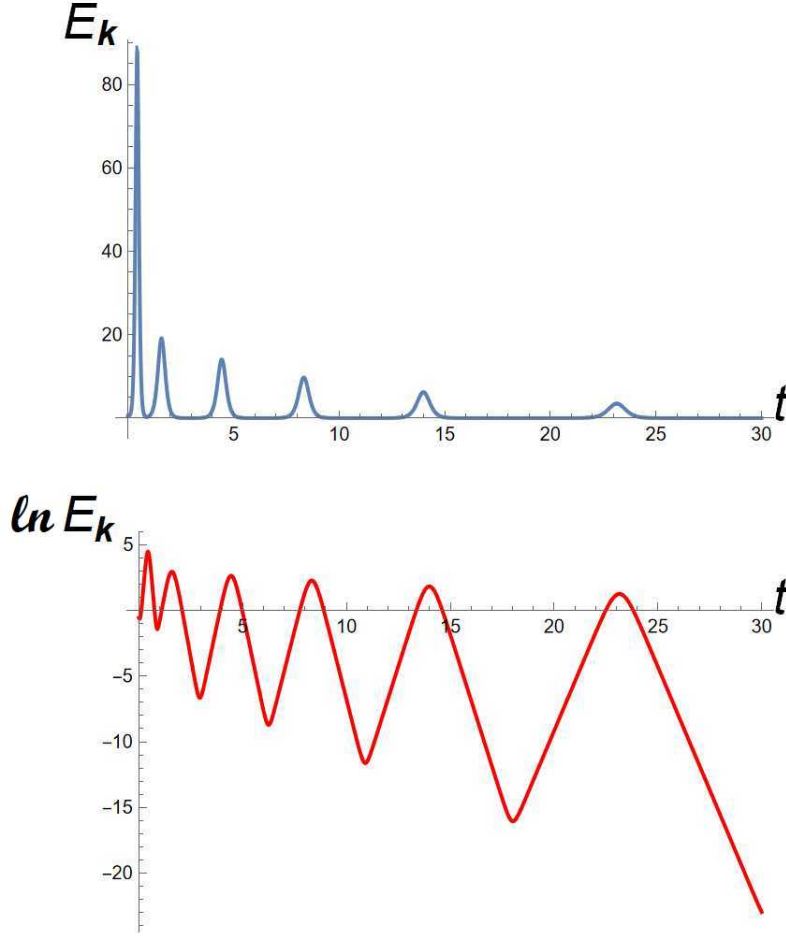


FIG. 3. The kinetic energy as a function of time parameter t . On the upper graph, apparently, E_k systematically reaches zero corresponding to the surface of the cone, and stays at this level for a long time, but the logarithmic scale in the lower graph reveals its oscillatory behaviour with reflections from the hyperboloidal surfaces (35).

- The instability of the exact solution on the anisotropic approach to collapse relies on growth of the ratio between the perturbation and unperturbed scale factors (rather than the growth of the perturbation itself). This conclusion was already presented in [8]. Reversing the time arrow, we obtain the conclusion that the universe would undergo isotropisation in a stable process.
- The final point at $t \rightarrow \infty$ is always the apex. Since the exact solution is unstable, it cannot be an attractor. Bearing in mind that the only approach to the apex along a differentiable curve is that of the exact solution, we come up to the conclusion that the generic approach to the limit has no limit of the ratios between the scale factors. This infers that it is chaotic.
- The cone in the velocity space, corresponding to zero kinetic energy, together with the

hyperboloids of constant E_k prove to make a natural and useful tool for analysing the BKL equations. This is likely to extend to other Lagrangian systems with quadratic kinetic part.

Appendix A PROOF THAT THE EXACT SOLUTION IS THE ONLY DIFFERENTIABLE APPROACH TO ALL-DIRECTION COLLAPSE

(proof of Proposition 8)

Proof. It is convenient to express (28) in terms of the y_i variables, $i = 1, 2, 3$ (18), as each of them, as well as their derivatives, have well-defined limits at the apex, namely $y_i \rightarrow -\infty, \dot{y}_i \rightarrow 0$. For $i = 2, 3$, we assume existence of two limits which define the paths of approach

$$g_{i1} := \lim_{t \rightarrow \infty} y_i/y_1 = \lim_{t \rightarrow \infty} \dot{y}_i/\dot{y}_1 = \lim_{t \rightarrow \infty} \ddot{y}_i/\ddot{y}_1 \quad (36)$$

(by de l'Hôpital's rule). The last pair of expression for the limits define the direction of approach to the apex in the cone. We are going to prove that their existence implies that the approach to the apex is asymptotically identical with that of the exact solution. In terms of the y_i variables the latter reads

$$y_1 = \ln \frac{9}{(t-t_0)^2}, \quad y_2 = \ln \frac{10}{(t-t_0)^2}, \quad y_3 = \ln \frac{4}{(t-t_0)^2}. \quad (37)$$

From equations (13)–(12), for $i = 2, 3$, we have

$$\begin{aligned} 0 \leq g_{21} &= \lim_{t \rightarrow \infty} \frac{y_2}{y_1} = \lim_{t \rightarrow \infty} \frac{\ddot{y}_2}{\ddot{y}_1} = \lim_{t \rightarrow \infty} \frac{2 \exp y_1 - 2 \exp y_2 + \exp y_3}{2 \exp y_2 - 2 \exp y_1}, \\ 0 \leq g_{31} &= \lim_{t \rightarrow \infty} \frac{y_3}{y_1} = \lim_{t \rightarrow \infty} \frac{\ddot{y}_3}{\ddot{y}_1} = \lim_{t \rightarrow \infty} \frac{\exp y_2 - 2 \exp y_3}{2 \exp y_2 - 2 \exp y_1}. \end{aligned} \quad (38)$$

The nonnegative property of g_{21} and g_{31} follows from $\forall_{i \in \{1,2,3\}} y_i \rightarrow -\infty$.

Consider the limit $\lim_{t \rightarrow \infty} 2y_2/y_1 + y_3/y_1$, first for $g_{21} < 1$

$$0 \leq g_{213} := 2g_{21} + g_{31} = \lim_{t \rightarrow \infty} \frac{-3 \exp y_2 + 4 \exp y_1}{2 \exp y_2 - 2 \exp y_1} = \lim_{t \rightarrow \infty} \frac{-3 + 4 \exp [y_1(1 - y_2/y_1)]}{2 - 2 \exp y_1(1 - y_2/y_1)} = -\frac{3}{2}. \quad (39)$$

If $g_{21} > 1$, then, by an analogous transformation, $g_{213} = -2$. Both results contradict the nonnegative property. Hence, $g_{21} = 1$.

For $g_{32} := \lim_{t \rightarrow \infty} y_3/y_2$, consider the sum of reciprocals

$$0 \leq g_{231} := \frac{1}{g_{21}} + \frac{1}{g_{31}} = \lim_{t \rightarrow \infty} \frac{\exp y_3}{\exp y_2 - 2 \exp y_3}. \quad (40)$$

If $g_{32} < 1$, then, by a similar transformation, $g_{231} := 1/g_{32} + 1/g_{31} = -\frac{1}{2}$, which contradicts the nonnegative property.

If $g_{32} > 1$, then we obtain in a similar way, $g_{231} = 0$. However, this is impossible since $g_{21} = 1$ and $g_{31} \geq 0$. As a result, both g_{21} and g_{31} must be equal to 1. Substituting these limits to (38), we obtain, after simple manipulation

$$\lim_{t \rightarrow \infty} \frac{\exp y_3}{\exp y_2 - \exp y_1} = 4 \quad \text{and} \quad \lim_{t \rightarrow \infty} \frac{\exp y_2}{\exp y_2 - \exp y_1} = 10, \quad (41)$$

which entails

$$\lim_{t \rightarrow \infty} (y_2 - y_1) = \ln \frac{10}{9}, \quad \lim_{t \rightarrow \infty} (y_3 - y_1) = \ln \frac{4}{9}. \quad (42)$$

Finally, the asymptotic time dependence may be recovered from (21), which in terms of y_i has the form

$$\frac{3}{4}\dot{y}_1^2 + 2\dot{y}_1\dot{y}_2 + \dot{y}_2^2 + \dot{y}_1\dot{y}_3 + \dot{y}_2\dot{y}_3 - \frac{9}{2}\ddot{y}_1 - 5\ddot{y}_2 - 2\ddot{y}_3 = 0. \quad (43)$$

Dividing both sides of (43) by \dot{y}_1^2 and bearing in mind that all quotients \dot{y}_i/\dot{y}_1 and \ddot{y}_i/\ddot{y}_1 tend to 1, we obtain the asymptotic, which may be written as

$$\lim_{t \rightarrow \infty} \frac{d}{dt} \left(\frac{1}{\dot{y}_1} \right) = -\frac{1}{2}, \quad (44)$$

Integrating, we get the asymptotic of y_1 in the neighbourhood of $t = \infty$

$$\dot{y}_1 = -2/(t - t_0), \quad y_1 = \ln \frac{C}{(t - t_0)^2}. \quad (45)$$

While the value of t_0 is arbitrary, the value of C may be recovered by substitution of (45) into the constraint (17), which yields $C = 9$. Subsequent substitutions, of this C into (45), and the resulting y_1 into (42), yield precisely the asymptotic of the exact solution. \square

Appendix B PROOF THAT ALL TRAJECTORIES EVENTUALLY TEND TO THE APEX

(proof of Proposition 10)

Proof. In Proposition 9, we proved $\gamma_1 = \gamma_2 = 0$, $\gamma_3 \leq 0$. We are going to prove that $\gamma_3 < 0$ is impossible.

Assume $\gamma_3 < 0$. Adding first two equations in the y_i -version of (13) (which corresponds to adding first two rows of matrix M), we obtain

$$\ddot{y}_1 + \ddot{y}_2 = \exp y_3. \quad (46)$$

Since $\lim_{t \rightarrow \infty} \dot{y}_3 = \gamma_3 < 0$, then for all $\varepsilon > 0$ a time T exists such that for all $t > T$, we have

$$\dot{y}_3 \in]\gamma_3 - \varepsilon, \gamma_3 + \varepsilon[, \quad \text{whence } y_3 - y_3(T) \in](\gamma_3 - \varepsilon)(t - T), (\gamma_3 + \varepsilon)(t - T)[. \quad (47)$$

Choose ε such that $\gamma_3 + \varepsilon < 0$. We have

$$\ddot{y}_1 + \ddot{y}_2 \in]e^{y_3(T) + (\gamma_3 - \varepsilon)(t - T)}, e^{y_3(T) + (\gamma_3 + \varepsilon)(t - T)}[, \quad (48)$$

with both exponents negative for large t . Hence

$$\dot{y}_1 + \dot{y}_2 \in]\frac{1}{\gamma_3 - \varepsilon}e^{y_3(T) + (\gamma_3 - \varepsilon)(t - T)} + C_1, \frac{1}{\gamma_3 + \varepsilon}e^{y_3(T) + (\gamma_3 + \varepsilon)(t - T)} + C_1[, \quad (49)$$

where C_1 is a constant of integration. Since $\gamma_1 = \lim_{t \rightarrow \infty} \dot{y}_1 = 0$ and $\gamma_2 = \lim_{t \rightarrow \infty} \dot{y}_2 = 0$ as $t \rightarrow \infty$ (Proposition 9), we have $C_1 = 0$. Then, integrating again (49), we obtain

$$y_1 + y_2 \in]\frac{1}{(\gamma_3 - \varepsilon)^2}e^{y_3(T) + (\gamma_3 - \varepsilon)(t - T)} + C_2, \frac{1}{(\gamma_3 + \varepsilon)^2}e^{y_3(T) + (\gamma_3 + \varepsilon)(t - T)} + C_2[, \quad (50)$$

where C_2 is a constant of the next integration. However the constraint (17) requires that both $y_1 \rightarrow -\infty$ and $y_2 \rightarrow -\infty$ as $t \rightarrow \infty$, while the limit of the r.h.s. is a finite number C_2 . Hence, the assumption $\gamma_3 < 0$ leads to a contradiction, whence $\gamma_3 = 0$.

The conclusion that all γ_i , $i = 1, 2, 3$ are equal to zero means that all trajectories eventually end at the apex. \square

-
- [1] V. A. Belinskii, I. M. Khalatnikov, and E. M. Lifshitz, “Oscillatory approach to a singular point in the relativistic cosmology”, *Adv. Phys.* **19**, 525 (1970) <https://doi.org/10.1080/00018737000101171>
 - [2] V. A. Belinskii, I. M. Khalatnikov, and E. M. Lifshitz, “A general solution of the Einstein equations with a time singularity”, *Adv. Phys.* **31**, 639 (1982) <https://doi.org/10.1080/00018738200101428>
 - [3] V. A. Belinskii, I. M. Khalatnikov, and M. P. Ryan, “The oscillatory regime near the singularity in Bianchi-type IX universes”, Preprint **469** (1971), Landau Institute for Theoretical Physics, Moscow; the part by V. A. Belinskii and I. M. Khalatnikov has been published as sections 1 and 2 in M. P. Ryan, *Ann. Phys.* **70**, 301 (1971) [https://doi.org/10.1016/0003-4916\(72\)90269-2](https://doi.org/10.1016/0003-4916(72)90269-2)
 - [4] V. A. Belinski, “On the cosmological singularity,” *Int. J. Mod. Phys. D* **23**, 1430016 (2014) <https://doi.org/10.1142/S021827181430016X>
 - [5] E. Czuchry and W. Piechocki “Bianchi IX model: Reducing phase space” *Phys. Rev. D* **87**, 084021 (2013) <https://doi.org/10.1103/PhysRevD.87.084021>
 - [6] E. Czuchry, N. Kwidzinski and W. Piechocki “Comparing the dynamics of diagonal and general Bianchi IX spacetime, *Eur. Phys. J. C* **79**:173 (2019) <https://doi.org/10.1140/epjc/s10052-019-6690-y>
 - [7] V. Belinski and M. Henneaux, *The Cosmological Singularity* (Cambridge University Press, Cambridge, 2017) <https://doi.org/10.1017/9781107239333>
 - [8] P. Goldstein and W. Piechocki, “Generic instability of the dynamics underlying the Belinski-Khalatnikov-Lifshitz scenario” *Eur. Phys. J. C* **82**:216 (2022) <https://doi.org/10.1140/epjc/s10052-022-10158-7>
 - [9] R.Conte, “On a dynamical system linked to the BKL scenario”, *Phys. Scr.* **98** 105212 (2023) <https://doi.org/10.1088/1402-4896/acf4d3>
 - [10] V. A. Belinski and I. M. Khalatnikov, “On the nature of the singularities in the general solution of the gravitational equations”, *Sov. Phys. JETP* **29**, 911 (1969); translation from Russian of *Zh. Eksp. Teor. Fiz.* **56**, 1701 (1969)
 - [11] P.P. Goldstein “A Quadric of Kinetic Energy in the Role of Phase Diagrams – Application to the Belinski-Khalatnikov-Lifshitz Scenario”, *Geometric Methods in Physics XL Workshop Białowieża, Poland*, P. Kielanowski et al. eds. (Birkhäuser 2024), p. 331 <https://doi.org/10.1007/978-3-031-62407-0>
 - [12] Ch.W. Misner, K.S. Thorne and J.A. Wheeler, *Gravitation* (W.H. Freeman & Co., San Francisco 1973), §30.2 and §30.7